Manipulating and Dispensing Micro/Nanoliter Droplets by Superhydrophobic Needle Nozzles

Zhichao Dong,[†] Jie Ma,[†,*] and Lei Jiang[†,§,*]

[†]Beijing National Laboratory for Molecular Sciences (BNLMS), Key Laboratory of Organic Solids, Institute of Chemistry, Chinese Academy of Sciences (ICCAS), Beijing, 100190, People's Republic of China and [§]School of Chemistry and Environment, Beihang University, Beijing, 100191, People's Republic of China

ABSTRACT There is rapidly increasing research interest focused on manipulating and dispensing tiny droplets in nanotechnology and biotechnology. A micro/nanostructured superhydrophobic nozzle surface is one promising candidate for the realization of tiny droplet manipulating applications. Here, we explore the feasibility of using superhydrophobicity for guided dispensing of tiny water droplets. A facile dip-coating method is developed to prepare superhydrophobic needle nozzles (SNNs) based on commercial needle nozzles with reduced inner diameter. The SNNs can manipulate tiny droplets of different volumes by only changing the inner diameter of the nozzle, rather than reducing the nozzle size as a whole. Different from the previous electric-field-directed process or pyroelectrodynamic-driven technique, quasi-stable water drops down to the picoliter scale can be produced by SNNs without employing any extra driving mechanisms. Due to their intrinsic superhydrophobic nature, the SNNs also possess the properties of reducing sample liquid retention, improving sample volume transfer accuracy, and saving expensive reagents. In addition, this kind of dip-coating method can also be applied to micropipet tips, inkjet or bioprinter heads, *etc*. As the issues of reducing drop size and increasing drop volume accuracy are quite important in the laboratory and industry, this facile but effective superhydrophobic nozzle-coating method for manipulating tiny droplets could be of great help to make breakthroughs in next-generation liquid transport and biometric and inkjet printing devices.

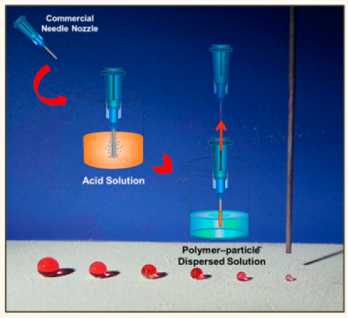

KEYWORDS: superhydrophobic surface · tiny droplet · dip-coating · nozzle · micro/nanostructures · surface modification

Manipulating and dispensing micro- or nanoliter liquids is of great interest for its wide applications in various fields, such as liquid transportation,[1−4] bioassays,[5−9] drug screening,[10,11] inkjet printing,[12−16] and lab experiments concerning predetermined volumes of tiny drops.[17−19] Over the past decades, numerous efforts from both scientific and industrial communities have been made to achieve smaller drops, by shrinking the nozzle size[7,17] or employing extra driving mechanisms, such as heat ejection,[20] electric-field-directed processes,[21,22,45,46] and pyroelectrodynamic-driven technique.[23] However, the existing inkjet printing or drop-on-demand techniques involve a lot of complex technical problems that require complicated devices to control high voltage, alternating current, gas flow, *etc*.[20−23,45,46] In addition, reducing the nozzle size down to micrometer scales not only reduces its mechanical properties but also results in nozzles too fragile for practical applications. Furthermore, obtaining tiny droplets by extra driving mechanisms usually results in high ejecting velocity, which is undesirable in many cases.[2] Obtaining quasi-stable tiny droplets in a facile and low-cost way is therefore still a challenge.

Nature gives us plenty of inspiration in designing novel functional materials, especially with special wetting properties,[25,26] for instance, the self-cleaning architecture inspired by the lotus leaf,[24] antifogging glass inspired by mosquito eyes,[27] and the highly adhesive glove inspired by gecko feet.[28−30] These phenomena provide us with important clues to realize that special wettabilities of solid surfaces could be realized through the cooperation of surface chemical composition and micro/nanostructures.[32] In recent decades, bioinspired micro/nanostructured superhydrophobic surfaces have been intensively investigated.[24,31] For such a superhydrophobic surface, according to the Cassie–Baxter model, air is trapped in the rough area, and water is in physical contact only with the peaks in roughness created by the film.

* Address correspondence to jianglei@iccas.ac.cn; majie@iccas.ac.cn.

Received for review September 13, 2013 and accepted October 11, 2013.

Published online October 11, 2013
10.1021/nn4048099

This type of air entrapment, called plastron, has been shown to reduce water adhesion to the superhydrophobic surface.[34] Recently, our group reported that the lotus rims can be used as antioverflowing edges.[37] This kind of superhydrophobic rim could avoid water flowing over the upper surface, so lotus leaves float on water rather than sink into the water. Inspired by the superhydrophobic rim, novel strategies to construct superhydrophobic edges, such as microconvexes and microgrooves, were used to restrict the spreading of water drops.[1,35,36,44]

Here, inspired by the superhydrophobic lotus rims, we use the concept of the superhydrophobic edge effect to control the size of dispensed droplets. In our experiment, superhydrophobic needle nozzles (SNNs) are prepared based on commercially available needle nozzles by a facile polymer/particle dip-coating process. The inner diameter of the needle nozzle can be tuned simply through changing the dip-coating times. Due to their intrinsic superhydrophobic edge effect, the superhydrophobic inner edge of the SNNs can effectively restrict the spreading of a pendulous water droplet, and the volume of a droplet ejected from the SNNs is related to the inner diameter. In this way, quasi-stable droplets down to picoliter scale can be acquired by SNNs without the need of sophisticated circuits, electronic boards, or extra driving forces. This method can be used to reinvent functional droplet-dispensing devices in a facile way and in addition to provide a unique platform for manipulating pico- to microliter droplets with relevance to biology and inkjet printing.

RESULTS AND DISCUSSION

The process to prepare the micro/nanostructured superhydrophobic nozzle-surface is schematically illustrated in Figure 1A. Common hydrophobic steel needle nozzles ($D_o = 500\ \mu m$, $D_i = 350\ \mu m$) were used as the base material for further modification. In detail, two steps were involved to endow the hydrophobic steel needle nozzle with micro/nanostructured superhydrophobicity: First, the hydrophobic steel needle nozzles were immersed into a nitric acid (HNO_3) and hydrochloric acid (HCl) mixture solution to achieve a microstructured morphology. In this acid-etching step, hydrogen gas was indeed a byproduct of acid etching, but it can selectively protect the ferric substrate at sites covered by the bubbles, achieving the microstructures simultaneously with the etching of iron. By adjusting the etching time, we can achieve the corresponding surface morphology, as shown in Figure 1B,D. Second, the microstructured nozzle was dipped into a polymer–particle dispersed solution (commercial hydrophobic polymer and hydrophobic fumed silica nanoparticles) for nanoparticle coating, finally achieving the micro/nanostructured morphology (Figure 1C,E). In this dip-coating step, the hydrophobic fumed silica particles can create nanostructured surface textures, and the commercial hydrophobic polymer can reduce the surface energy.[2] Both of the above are necessary for superhydrophobic surfaces with a low water adhesive property.[24,25] The as-prepared micro/nanostructured nozzle surface, without being modified by any fluoroalkyl silanes, exhibited a water contact angle (CA) as high as 165.3 ± 5.2° and a water sliding angle less than 3°. The characterization of adhesive force (22.3 ± 3.2 μN) also proves that the SNN is low-adhesive (data tested on a flat surface with the same processing procedures).

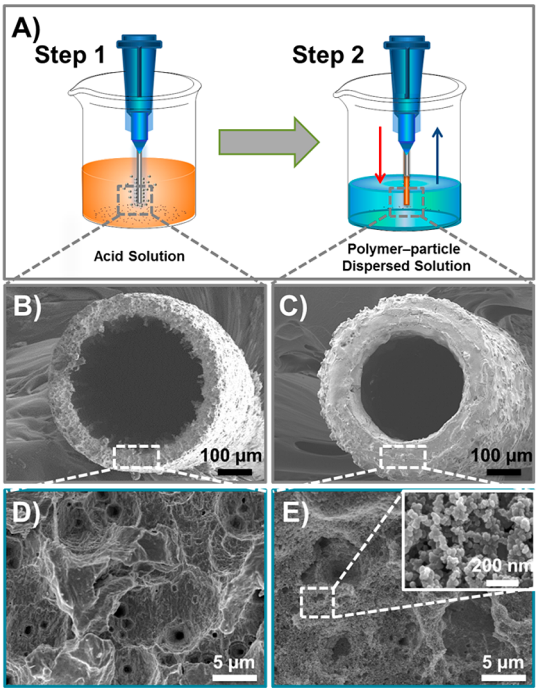

Figure 1. Construction strategy and morphology of the superhydrophobic needle nozzles (SNNs). (A) Scheme of the two-step formation process using commercial needle nozzles to prepare SNNs. Step 1 and step 2 represent the acid-etching method and dip-coating method, respectively. Repeating step 2 can reduce the inner diameter of the SNNs. Large-area scanning electron microscope (SEM) image of the surface of (B) microstructured nozzle tip prepared by acid etching and (C) micro/nanostructured nozzle tip prepared by dip-coating. (D, E) Enlarged SEM views of B and C, respectively. (Inset in E) Enlarged SEM image of the nanostructured morphology.

As a control experiment, we also prepared two other types of needle nozzles with the same dimension (D_o = 500 μm, D_i = 350 μm) but different wetting properties: hydrophilic nozzles and hydrophobic nozzles. In brief, the hydrophilic needle nozzle was prepared by dipping the commercial needle nozzle into the acid mixture solution. The hydrophobic nozzles were achieved by fluorinating the commercial needle nozzle with 1*H*,1*H*,2*H*,2*H*-perfluorodecanethiol. The as-prepared hydrophilic nozzle and hydrophobic nozzle displayed water CAs of 54.5 ± 4.6° and 112.5 ± 8.3° and water adhesive forces of 99.4 ± 12.3 and 77.2 ± 9.4 μN, respectively (Figure 2).

In order to investigate the influence of wettability and size of nozzles on the volume of separating drops,

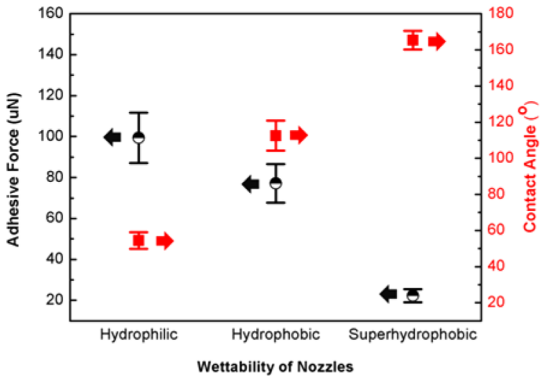

Figure 2. Wetting property of the nozzle surfaces. Water adhesive force and the water contact angle of the nozzle-tip surface with different wettability: hydrophilic, hydrophobic, superhydrophobic. The contact angles and adhesives forces are tested on the corresponding planar substrates, which were prepared by using the same materials and processing methods as those of needle nozzles, instead of the sub-millimeter scaled nozzle tips, which were too tiny to test on.

these three kinds of needles were connected to glass syringes (1.0 mL) that are already filled with distilled water and driven by an electrical microinjection pump. The injection speed of the electrical microinjection pump was set at 0.25 μL/s to dispense microliter droplets (droplet volume >1 μL) and 0.01 μL/s to dispense nanoliter or picoliter droplets (droplet volume <1 μL). In our experiment, the dimensionless Weber number, $We = \rho v^2 D/\sigma$, corresponding to a water liquid with surface tension σ, density ρ, linear injection speed v, and diameter of a nozzle D, was less than 10^{-5}. This ensured that the injection speed has no influence on the volume of ejected droplets.

The relationship between the volume of the quasi-stable droplet and the wettability of the nozzles is shown in Figure 3. For the hydrophilic nozzle, water would overflow the outer wall. For the hydrophobic nozzle, a pendulous droplet was pinned at the outer edge of the nozzle (contact area = $\pi D_o^2/4$). The difference between these two phenomena is mainly caused by the different wetting properties. Because the hydrophilic nozzle has a higher apparent surface energy than the hydrophobic nozzle, water would be more easily driven by the capillary force to cling on the outer wall of the hydrophilic needle nozzle. With the process of pumping proceeding, the volume of a pendulous droplet would grow until the pendulous droplet has undergone a sudden transition to a dripping droplet state. To put it in another way, the pendulous drop would not detach from the nozzle until the gravity of the growing drop was higher than the maximum adhesive force that the nozzle-tip surface can provide (Figure 3B,D).[38,39] Since the water adhesive force of the hydrophilic nozzle surface is higher than that of the hydrophobic nozzle surface, the size of the droplet drips from the hydrophilic nozzle (9.8 $\pm$ 0.6 μL, $We = 4.0 \times 10^{-7}$) is larger than that separating from the hydrophobic nozzle (7.3 $\pm$ 0.8 μL, $We = 4.0 \times 10^{-7}$).

For the SNNs, as shown in Figure 3E, because the superhydrophobic edge brings strong restrictions against water overflowing onto the superhydrophobic nozzle-tip surface, the contact line did not move away from the inner edge of the nozzle-tip surface. As displayed in Figure 3F, the dynamic water contact angle ($\theta_4 > \theta_3 > \theta_2 > \theta_1$) between the droplet and the nozzle surface increased with increasing ejecting volume. In addition, gravity would drag the drop off the nozzle before the advancing contact angle of the SNNs surface (nearly 180°) is achieved during the injection process. Thus, the contact line of the drop is always pinned at the inner edge of the nozzle tip before the pendulous droplet separates from the SNN. Due to the low water adhesive force (22.3 μN) and low contact area between the pendulous droplets and the superhydrophobic surface, the average volume (2.4 $\pm$ 0.3 μL, $We = 4.0 \times 10^{-7}$) of the droplets detached from the micro/nanostructured SNNs was dramatically reduced to only a quarter of that separated from the hydrophilic nozzle (9.8 $\pm$ 0.6 μL, $We = 4.0 \times 10^{-7}$).

The volume of the quasi-stable droplet is also related to the dimension of the nozzles used. For the hydrophobic and the hydrophilic nozzle, as plotted in Figure 4A,B, the volume of the dripping droplet decreased with the narrowing of the outer radius (D_o), but stayed the same when altering the inner diameter without changing the outer diameter. This means that the only way to eject tiny water droplets from a hydrophobic or a hydrophilic nozzle is to reduce its whole size. However, it is rather costly to achieve an ultrathin nozzle. In comparison, for the SNNs, the contact line of the drop is always pinned at the inner edge of the nozzle tip, and the volume of the droplet is related only to the inner diameter of superhydrophobic nozzles. It is thus possible to achieve small droplets from a common sized nozzle by introducing superhydrophobicity and reducing the inner diameter of a commercialized needle nozzle simultaneously.

Theoretically, the volume of a quasi-stable droplet that eventually separates from the SNN surface is mainly determined by competition between the gravity of the pendulous droplet and the dragging force provided by the nozzle. The liquid's surface tension σ, the liquid's viscosity μ, and the nozzle's dimension are all important factors in determining the dragging force. In our experiments, the Ohnesorge number ($Oh = \mu/(\rho\sigma D)^{1/2}$, 20 °C) ranged from 8.85×10^{-3} to 37.06×10^{-3}, which is below 0.1, indicating that the influence of the liquid viscosity can be neglected.[40,41] Thus, in the case of the SNN, derived from its intrinsic superhydrophobicity, the dragging force is mainly provided by the vertical component of the capillary force ($\pi D_i \sigma \sin\theta$) between the pendulous droplet and the inner edge surface of the SNN. As shown in Figure 3F, by balancing the gravitational force and the capillary force in the case of the SNNs, the volume V of

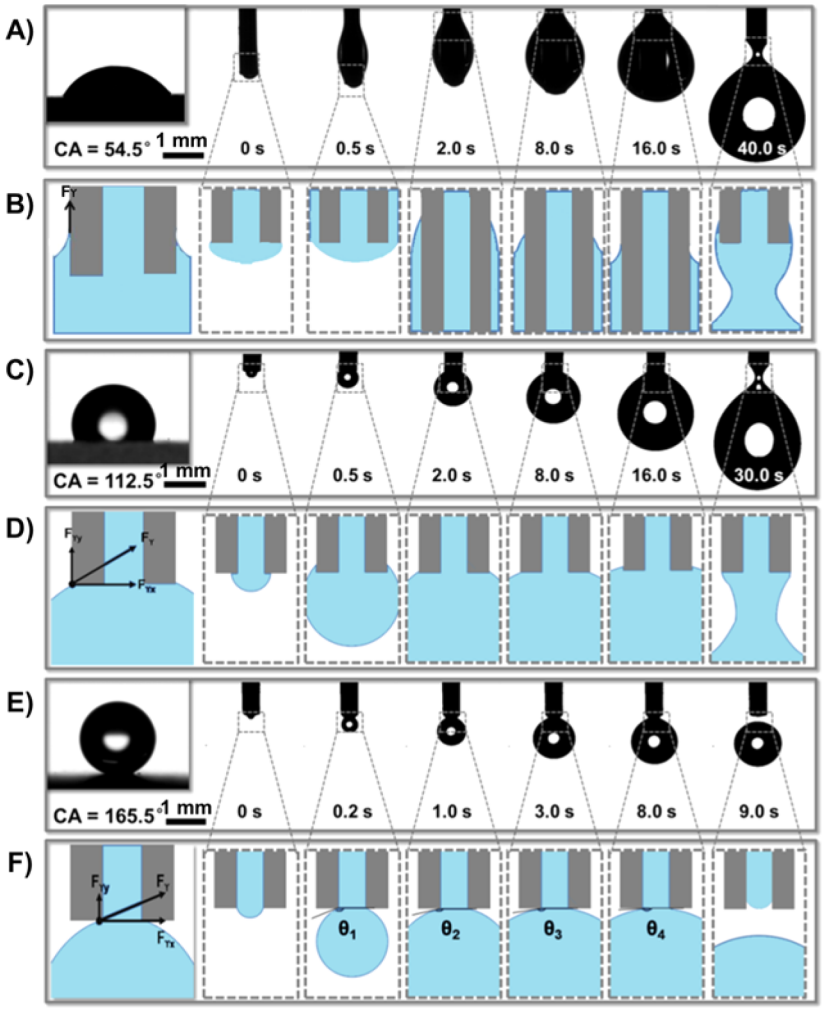

Figure 3. Correlation between the size of dripping droplets and the wetting property of the nozzles. (A, C, E) Left: the contact angles of water droplets on the surfaces of as-prepared substrates by using the same materials and treatment processes as these needle nozzles, respectively. Right: Photographs of the droplets that are dripping from the tip of (A) hydrophilic needle nozzle, (C) hydrophobic needle nozzle, and (E) superhydrophobic needle nozzle. (B, D, F) Left: Schematic diagram of the mechanical analysis: the size of the dripping droplet was determined by the vertical component of the capillary force and the gravity of the pendulous droplet. Right: The contact line is pinned at the outer edge for the hydrophobic nozzle and at the inner edge (dynamic contact angle: $\theta_4 > \theta_3 > \theta_2 > \theta_1$) for the superhydrophobic nozzle.

the dripping drop varies with the inner diameter D_i and the detaching contact angle θ, which can be expressed as

$$V = \frac{\pi\sigma D_i \sin\theta}{\rho g} \quad (1)$$

Here, g is the gravitational acceleration. From eq 1, we can find that the volume of the dripping droplet ejected from the SNNs was determined by the property of the liquid (σ/ρ), the inner diameter of the nozzle-hole (D_i), and the liquid detaching contact angle (θ). Thus, the theoretical volume (V) of the dripping water droplet (σ/ρ = constant) is in direct proportion to the water detaching contact angle (θ) and the inner diameter of the SNN (D_i):

$$V \propto D_i \sin\theta \quad (2)$$

Changing the inner diameter of the SNNs is possible by dip-coating the polymer thin film onto the inner wall of the acid-etched nozzles. Experimentally, the narrowing of the inner diameter of the SNNs from 350 μm to 20 μm can be achieved by changing the dip-coating repetition times. In detail, when the acid-etched hydrophilic nozzle was immersed into the polymer−particle dispersed solution, the capillary force could drive the solution to wet the inner wall of the nozzle (Figure S1 in the Supporting Information). After pulling the wetted nozzle from the solution, heating could accelerate the evaporation of solvent and solidify the polymer/particle coating. Repeating the dipping times could increase the thickness of the polymer/particle coating, which could simultaneously lead to the reduction of the inner diameter of the SNNs. As shown in Figure 4C, the thickness of the polymer/particle coating increased nearly 20 μm per dip-coating cycle. In addition, our approach is general to a broad range of materials including plastics and metal, such as plastic micropipet tips and copper heads. These nozzles

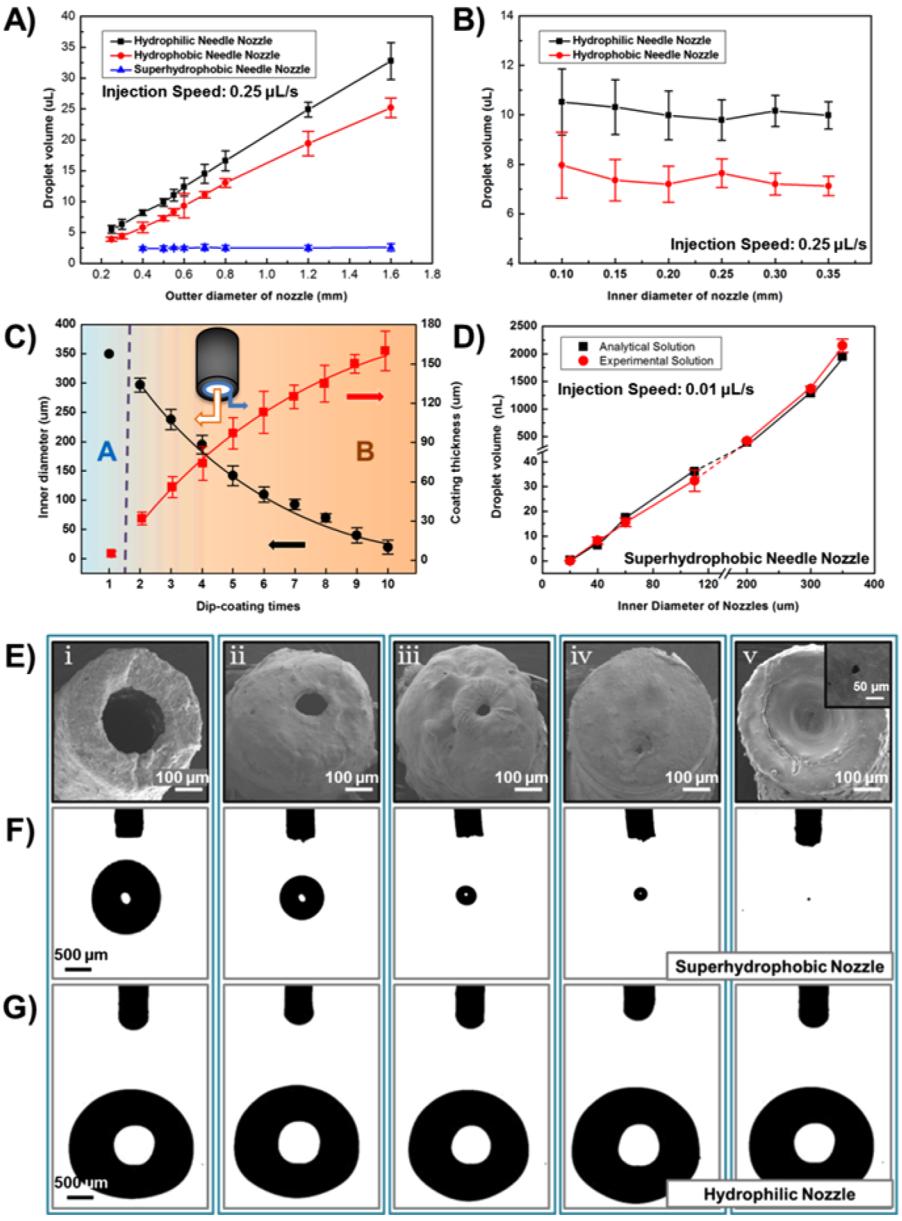

Figure 4. Correlation between the volume of dripping droplets and the size of nozzles. (A) The volume is related to the outer diameter (D_o) of the hydrophobic needle nozzle or the hydrophilic needle nozzle, but unrelated to that of SNNs. (B) The volume of dripping droplets stays almost unchanged when reducing the inner diameter of the hydrophobic or hydrophilic nozzle, while the outer diameter of these nozzles stays the same at 500 μm. (C) The thickness of the polymer−particle coating or the inner diameter of the nozzle is related to the dip-coating times. The thickness of the polymer−particle coating increases nearly 20 μm per one dip-coating time. In A, the dipping speed is 40 mm/s and the pulling speed is 40 mm/s. In B, the dipping speed is 80 mm/s and the pulling speed is 100 mm/s. (D) Analytical and experimental data of the volume of the dripping droplets from SNNs with different inner diameters: the volume of the dripping droplets is almost in direct proportion to the inner diameter of SNNs. (E) Large-area SEM images of the micro/nanostructured nozzle with an outer diameter of 500 μm and inner diameter of (i) 350 μm, (ii) 200 μm, (iii) 110 μm, (iv) 40 μm, and (v) 20 μm, respectively. (v) Inset is the enlarged SEM images of the nozzle hole. (F) Optical images of the quasi-stable droplets ejected from the SNNs with a volume of (i) 2400.0 nL, (ii) 420.0 nL, (iii) 22.4 nL, (iv) 8.2 nL, and (v) 0.1 nL, respectively. (G) After treating with O_2 plasma, the volume of the quasi-stable droplets changed to (i) 9860.0 nL, (ii) 9940.0 nL, (iii) 9650.0 nL, (iv) 10400 nL, and (v) 9980.0 nL.

can also be treated with this dip-coating method to modify the nozzle surface with micro/nanostructured superhydrophobicity (Figure S2 in the Supporting Information).

To test the capability of the SNNs to dispense microsized liquid droplets with controllable volume, as shown in Figure 4E, we fabricated a series of SNNs with inner diameters of 350, 200, 110, 40, and 20 μm, with the same outer diameter. For each nozzle size, the injection speed was set at 0.01 μL/s ($6.3 \times 10^{-10} < We < 3.4 \times 10^{-6}$). Experimentally, the volume of the dripping droplet is almost in direct proportion to the inner diameter D_i of the SNNs, and the results are plotted in Figure 4D. Significantly, the experimental result agrees well with the theoretical one calculated from eq 1.

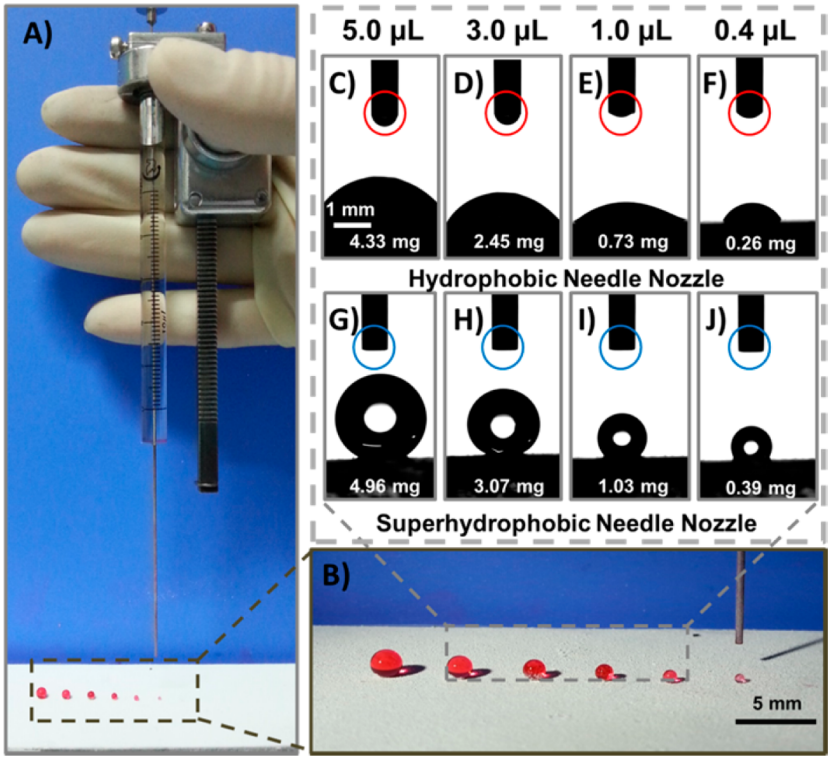

Figure 5. Application of the SNNs: accurate manipulation of droplets, low liquid retention, high delivery efficiency, and no cross contamination. (A) Photograph of the droplet-ejecting process by simply using a microliter syringe. (B) Enlarged image of the droplets with different volumes ejected by the microliter syringe equipped with a superhydrophobic needle nozzle. Microliter syringes with (C–F) a hydrophobic needle nozzle and (G–J) a superhydrophobic needle nozzle were used to dispense water droplets of 5.0, 3.0, 1.0, and 0.4 μL, respectively. For the hydrophobic needle nozzle, the pendulous drop cannot fall freely itself. A hydrophilic flat glass slide is used to contact and drag the pendulous droplet to separate it from the nozzle. After the contacting process, residual water inevitable clings to the tip of the hydrophobic needle nozzle. For superhydrophobic needle nozzles, water droplets fall freely from the tip of such nozzles, and no residual water is left. A microbalance is used to prove the SNNs with low retention property. Dispensing tiny drops by the SNNs can not only effectively reduce liquid retention and give high precision but also increase delivery speed and prevent contamination issues without touching the nozzle to the surface being dispensed to.

Thus, we can theoretically and experimentally demonstrate that shrinking the inner diameter of the SNNs, rather than shrinking the nozzle as a whole, leads to a reduction of drop size (Figure 4E,F). In order to further prove the capability of the SNNs to produce tiny droplets derived from their intrinsic superhydrophobic edge effect, we used the O_2 plasma etching method to change the wettability of the SNN surface to hydrophilicity without changing the inner diameter. As a result, the volumes of the dripping droplets (10 μL) became at least 4 times larger (Figure 4G). Overall, by introducing superhydrophobicity to the nozzle and by reducing the size of the inner diameter through dip-coating without shrinking the overall size of the nozzle itself, we can reduce the volume of the ejected liquid droplets in a low-cost and easy way.

As shown in Figure 4F and Movie 1 in the Supporting Information, we can use our superhydrophobic nozzles (D_o = 500 μm, D_i = 20 μm) to obtain 100 picoliter water droplets (We = 3.38 × 10^{-6}). The volume of such a dripping droplet is comparable to the volume of the droplet ejected from a commercial high-resolution inkjet printer (50–200 pL) in a high ejecting velocity. As far as we know, this is the smallest free-falling droplet ever achieved in such a low ejecting velocity (in a quasi-stable state). In comparison with other tiny-droplet-dispensing methods,[20–23] this kind of superhydrophobic modification method not only increases the robustness of the nozzle but also reduces the complexity of nozzle fabrication as well as the cost of the driving system.

The SNNs can effectively reduce liquid retention at the opening, as shown in Figure 5, which may be beneficial for practical applications, such as manipulating accurate liquid volume, increasing delivery efficiency, and reducing cross contamination. For a commercial needle nozzle, when the volume of the pendulous water droplets is below 10 μL, no drops can be separated from the nozzle-tip surface freely. In this case, we had to use this kind of nozzle to contact the surface to dispense the droplet. Additionally, after dispensing the droplet, it is inevitable that a certain amount of liquid clings to the surface of the hydrophobic nozzle tip, which would cause the volume of the dispensed droplet to be inaccurate, as shown in Figure 5C–F. A microbalance was also used to quantify the mass loss of the droplets dispensed by the hydrophobic nozzle. In our experiment, when we dispensed a 0.4 μL water droplet, the volume

loss of the droplet is almost 53%, as shown in Figure 5F. Reducing liquid retention and manipulating accurate volume droplets has been a persisting problem in scientific and industrial fields.[42,43] In comparison, as shown in Figure 5G–J, water droplets fall freely from the tip of SNNs, and almost no residual water is left on the nozzle tip. Free-falling droplets also contribute to liquid transfer in a noncontact way. That is, the sample is dispensed without contacting the liquid or surface it is being dispensed to. In addition, the volume loss of the dispensed droplet is less than 1%. Thus, using the SNNs to manipulate droplets can not only give high precision but also increase delivery speed and effectively prevent contamination. In this way, small amounts of reactants or aqueous solutions could also be dispensed in a facile way by the SNNs without liquid retention.

CONCLUSION

In conclusion, we developed a novel concept of using a superhydrophobic nozzle for guided dispensing of tiny droplets. A facile polymer/particle dip-coating approach is explored to create a superhydrophobic needle nozzle that can produce tiny droplets down to picoliter volume. The volume of the dispensed droplets is related to the inner diameter of the SNNs, rather than the outer diameter for commonly available commercial nozzles. Simultaneously, the dimension of the inner diameter can be controlled by the number of dip-coating repetitions. The surface superhydrophobicity and shrunken inner diameter together contributed to a remarkable reduction in the volume of the dripping droplets. Using this method, we demonstrated that the prepared SNNs can manipulate tiny droplets of varied volumes, improve sample volume transfer accuracy, and reduce sample liquid retention, which helps save expensive reagents. We hope our polymer/particle nozzle-coating method will contribute to promote existing applications and reduce costs in liquid transport and biometric and inkjet printing applications.

EXPERIMENTAL SECTION

Materials. Unbeveled blunt-tip hypodermic steel needles with an inner diameter of 350 μm and an outer diameter of 500 μm were obtained from Aisiai Inc. The Capstone ST-200 polymer solution and hydrophobic fumed silica nanoparticles (Aerosil R202, average particle size 14 nm) used to construct the hierarchical structure are commercial products and are made by DuPont and Evonik Degussa Co. respectively. The 1*H*,1*H*,2*H*,2*H*-perfluorodecanethiol was purchased from Sigma-Aldrich. Hydrochloric acid and nitric acid were used as received. Ethanol and acetone were distilled before using. The hydrophobic needle nozzle was prepared by fluorinating a commercial needle nozzle with 0.01 M 1*H*,1*H*,2*H*,2*H*-perfluorodecanethiol in ethanol for 2 h, and the hydrophilic needle nozzle was achieved by dipping the commercial needle nozzle into an 8 M hydrochloric acid/4 M nitric acid mixture solution for 1 min.

Fabrication of the SNNs. The commercial needle nozzles used in our work were first cleaned with acetone, ethanol, and deionized water, successively. The polymer–particle dispensed solution was prepared by adding 1.0 g of hydrophobic fumed silica nanoparticles and 3 mL of Capstone ST-200 solution into 17 mL of acetone. The precleaned nozzles were first etched with an 8 M hydrochloric acid/4 M nitric acid mixture solution for 2 min to achieve the microsturctured morphology. After that, the acid-etched nozzles were dipped into polymer–particle dispensed solution at a speed of 40 mm/s and immersion depth of 2.5 mm, held for 30 s, and pulled up at a speed of 40 mm/s by a WPTL dip coater (MTI Co.) at 30 °C. Finally, the coated needle nozzles were heated on a hot plate at 120 °C (Thermo Scientific Co.) for 30 min and then heated at 80 °C in an oven for 1 h. In this step, the thickness of the polymer–particle coating was less than 5 μm. Adjusting the dipping or pulling speed and dipping times can narrow the inner diameter of the nozzle from 350 μm to 20 μm. To shrink the inner diameter of the SNNs or increase the thickness of the polymer–particle coating, the parameters were reset as dipping speed = 80 mm/s, immersion depth = 2.5 mm, holding time = 10 s, and pulling speed = 100 mm/s. After each dip-coating process, thermal treatment is a necessary step. In brief, the coated needle nozzles were heated on a hot plate at 120 °C for 5 min. Repeating the dipping times could increase the thickness of the polymer/particle coating, which could simultaneously lead to the reduction of the inner diameter of the SNNs, and the thickness of the polymer/particle coating was increased nearly 20 μm per dip-coating cycle.

Instruments and Characterizations. SEM images were measured with a field-emission scanning electron microscope at 10 kV (Hitachi S-4800, Japan). CAs were measured on a OCA 20 machine (Germany) at ambient temperature. The CA values were obtained by measuring more than five different positions on the corresponding planar substrates, which were prepared by using the same materials and processing methods as those of the needle nozzles, instead of the submillimeter scaled nozzle tips, which were too tiny to test on. The adhesive force was measured by removing a 10 μL droplet from the corresponding planar substrates by using a high-sensitivity microelectromechanical balance system with a resolution of 10 μg (DataPhysics DCAT 11, Germany) and a charge-coupled device (CCD) camera system at ambient temperature. A high-speed camera (Olympus Co., Japan) equipped with a 5× lens was used to capture the motion of the drop-dispensing process at frame rate up to 10 kfps. The dripping of droplet was driven by an electrical microinjection pump equipped on the OCA 20 machine (Germany), and the injection speed was controlled by OCA 20 software. In our experiment, we set the injection speed of the electrical microinjection pump at 0.25 μL/s to dispense microliter droplets and 0.01 μL/s to dispense nanoliter or picoliter droplets, which were comparatively low pushing speeds ($6.3 \times 10^{-10} < We < 3.4 \times 10^{-6}$) for these nozzles to make corresponding water droplets separate from the nozzle tip. The detachment of water droplets from the nozzle was in a quasi-stable state.

Conflict of Interest: The authors declare no competing financial interest.

Acknowledgment. This research is supported by the National Research Fund for Fundamental Key Projects (2012CB934101, 2012CB933202, 2013CB933000), National Natural Science Foundation (21121001, 91127025), and the Key Research Program of the Chinese Academy of Sciences (KJZD-EW-M01).

Supporting Information Available: Characterization of the geometry of the cross section of the polymer/particle coating on the as-prepared inner side of the SNNs. Optical images and SEM images of the superhydrophobic micropipet tip and the superhydrophobic bioprinter head, which are prepared by the dip-coating process based on a commercial plastic micropipet tip and copper heads. The video of droplet repetitions of the superhydrophobic needle nozzle. This material is available free of charge *via* the Internet at http://pubs.acs.org.

REFERENCES AND NOTES

1. Duncombe, T. A.; Erdem, E. Y.; Shastry, A.; Baskaran, R.; Boehringer, K. F. Controlling Liquid Drops with Texture Ratchets. *Adv. Mater.* **2012**, *24*, 1545–1550.
2. Su, B.; Wang, S. T.; Song, Y. L.; Jiang, L. A Miniature Droplet Reactor Built on Nanoparticle-Derived Superhydrophobic Pedestals. *Nano Res.* **2011**, *4*, 266–273.
3. Mertaniemi, H.; Jokinen, V.; Sainiemi, L.; Franssila, S.; Marmur, A.; Ikkala, O.; Ras, R. H. A. Superhydrophobic Tracks for Low-Friction, Guided Transport of Water Droplets. *Adv. Mater.* **2011**, *23*, 2911–2914.
4. Zhao, Y.; Fang, J.; Wang, H.; Wang, X.; Lin, T. Magnetic Liquid Marbles: Manipulation of Liquid Droplets Using Highly Hydrophobic Fe_3O_4 Nanoparticles. *Adv. Mater.* **2010**, *22*, 707–710.
5. Saunders, R. E.; Gough, J. E.; Derby, B. Delivery of Human Fibroblast Cells by Piezoelectric Drop-on-Demand Inkjet Printing. *Biomaterials* **2008**, *29*, 193–203.
6. Calvert, P. Materials Science. Printing Cells. *Science* **2007**, *318*, 208–209.
7. Loh, O.; Lam, R.; Chen, M.; Moldovan, N.; Huang, H.; Ho, D.; Espinosa, H. D. Nanofountain-Probe-Based High-Resolution Patterning and Single-Cell Injection of Functionalized Nanodiamonds. *Small* **2009**, *5*, 1667–1674.
8. Robinson, W. H.; DiGennaro, C.; Hueber, W.; Haab, B. B.; Kamachi, M.; Dean, E. J.; Fournel, S.; Fong, D.; Genovese, M. C.; de Vegvar, H. E. N.; *et al*. Autoantigen Microarrays for Multiplex Characterization of Autoantibody Responses. *Nat. Med.* **2002**, *8*, 295–301.
9. Xu, J. H.; Luo, G. S.; Li, S. W.; Chen, G. G. Shear Force Induced Monodisperse Droplet Formation in a Microfluidic Device by Controlling Wetting Properties. *Lab Chip* **2006**, *6*, 131–136.
10. Rene, A.; Cugnet, C.; Hauchard, D.; Authier, L. Elaboration of Screen-Printed Microelectrodes Working as Generator/Collector and Their Use in a Flow Cell System. *Sens. Actuators, B* **2012**, *174*, 225–230.
11. Dinon, A. Z.; Prins, T. W.; van Dijk, J. P.; Arisi, A. C. M.; Scholtens, I. M. J.; Kok, E. J. Development and Validation of Real-Time PCR Screening Methods for Detection of Cry1A.105 and Cry2Ab2 Genes in Genetically Modified Organisms. *Anal. Bioanal. Chem.* **2011**, *400*, 1433–1442.
12. Gosalia, D. N.; Diamond, S. L. Printing Chemical Libraries on Microarrays for Fluid Phase Nanoliter Reactions. *Proc. Natl. Acad. Sci. U.S.A.* **2003**, *100*, 8721–8726.
13. MacBeath, G.; Schreiber, S. L. Printing Proteins as Microarrays for High-Throughput Function Determination. *Science* **2000**, *289*, 1760–1763.
14. Ridley, B. A. All-Inorganic Field Effect Transistors Fabricated by Printing. *Science* **1999**, *286*, 746–749.
15. Zhang, L.; Liu, H.; Zhao, Y.; Sun, X.; Wen, Y.; Guo, Y.; Gao, X.; Di, C. A.; Yu, G.; Liu, Y. Inkjet Printing High-Resolution, Large-Area Graphene Patterns by Coffee-Ring Lithography. *Adv. Mater.* **2011**, *24*, 436–440.
16. Kang, B.; Min, H.; Seo, U.; Lee, J.; Park, N.; Cho, K.; Lee, H. S. Directly Drawn Organic Transistors by Capillary Pen: A New Facile Patterning Method using Capillary Action for Soluble Organic Materials. *Adv. Mater.* **2013**, *25*, 4117–4122.
17. Park, J. U.; Hardy, M.; Kang, S. J.; Barton, K.; Adair, K.; Mukhopadhyay, D. K.; Lee, C. Y.; Strano, M. S.; Alleyne, A. G.; Georgiadis, J. G.; *et al*. High-Resolution Electrohydrodynamic Jet Printing. *Nat. Mater.* **2007**, *6*, 782–789.
18. Choi, K. H.; Rahman, A.; Ko, J. B.; Rehmani, A.; Ali, A.; Doh, Y. H.; Kim, D. S. Development and Ejection Behavior of Different Material-Based Electrostatic Ink-Jet Heads. *Int. J. Adv. Manuf. Technol.* **2010**, *48*, 165–173.
19. Agresti, J. J.; Antipov, E.; Abate, A. R.; Ahn, K.; Rowat, A. C.; Baret, J. C.; Marquez, M.; Klibanov, A. M.; Griffiths, A. D.; Weitz, D. A. Ultrahigh-Throughput Screening in Drop-Based Microfluidics for Directed Evolution. *Proc. Natl. Acad. Sci. U.S.A.* **2010**, *107*, 4004–4009.
20. Darhuber, A. A.; Valentino, J. P.; Troian, S. M. Planar Digital Nanoliter Dispensing System Based on Thermocapillary Actuation. *Lab Chip* **2010**, *10*, 1061–1071.
21. Hong, J. S.; Lee, B. S.; Moon, D.; Lee, J.-G.; Kang, I. S. Pumpless Dispensing of a Droplet by Breaking up a Liquid Bridge Formed by Electric Induction. *Electrophoresis* **2010**, *31*, 1357–1365.
22. Huang, J. Y.; Lo, Y. C.; Niu, J. J.; Kushima, A.; Qian, X. F.; Zhong, L.; Mao, S. X.; Li, J. Nanowire Liquid Pumps. *Nat. Nanotechnol.* **2013**, *8*, 277–281.
23. Ferraro, P.; Coppola, S.; Grilli, S.; Paturzo, M.; Vespini, V. Dispensing Nano-Pico Droplets and Liquid Patterning by Pyroelectrodynamic Shooting. *Nat. Nanotechnol.* **2010**, *5*, 429–435.
24. Yao, X.; Song, Y.; Jiang, L. Applications of Bio-Inspired Special Wettable Surfaces. *Adv. Mater.* **2011**, *23*, 719–734.
25. Feng, L.; Li, S. H.; Li, Y. S.; Li, H. J.; Zhang, L. J.; Zhai, J.; Song, Y. L.; Liu, B. Q.; Jiang, L.; Zhu, D. B. Super-Hydrophobic Surfaces: From Natural to Artificial. *Adv. Mater.* **2002**, *14*, 1857–1860.
26. Li, X. M.; Reinhoudt, D.; Crego-Calama, M. What Do We Need for a Superhydrophobic Surface? A Review on the Recent Progress in the Preparation of Superhydrophobic Surfaces. *Chem. Soc. Rev.* **2007**, *36*, 1350–1368.
27. Gao, X.; Yan, X.; Yao, X.; Xu, L.; Zhang, K.; Zhang, J.; Yang, B.; Jiang, L. The Dry-Style Antifogging Properties of Mosquito Compound Eyes and Artificial Analogues Prepared by Soft Lithography. *Adv. Mater.* **2007**, *19*, 2213–2217.
28. Hansen, W. R.; Autumn, K. Evidence for Self-Cleaning in Gecko Setae. *Proc. Natl. Acad. Sci. U.S.A.* **2005**, *102*, 385–389.
29. Autumn, K.; Liang, Y. A.; Hsieh, S. T.; Zesch, W.; Chan, W. P.; Kenny, T. W.; Fearing, R.; Full, R. J. Adhesive Force of a Single Gecko Foot-Hair. *Nature* **2000**, *405*, 681–685.
30. Lee, H.; Lee, B. P.; Messersmith, P. B. A Reversible Wet/Dry Adhesive Inspired by Mussels and Geckos. *Nature* **2007**, *448*, 338–341.
31. Liu, K. S.; Jiang, L. Multifunctional Integration: From Biological to Bio-Inspired Materials. *ACS Nano* **2011**, *5*, 6786–6790.
32. Lee, D. J.; Kim, H. M.; Song, Y. S.; Youn, J. R. Water Droplet Bouncing and Superhydrophobicity Induced by Multiscale Hierarchical Nanostructures. *ACS Nano* **2012**, *6*, 7656–7664.
33. Krumpfer, J. W.; McCarthy, T. J. Dip-Coating Crystallization on a Superhydrophobic Surface: A Million Mounted Crystals in a 1 cm^2 Array. *J. Am. Chem. Soc.* **2011**, *133*, 5764–5766.
34. Bobji, M. S.; Kumar, S. V.; Asthana, A.; Govardhan, R. N. Underwater Sustainability of the "Cassie" State of Wetting. *Langmuir* **2009**, *25*, 12120–12126.
35. Zhang, J.; Gao, X.; Jiang, L. Application of Superhydrophobic Edge Effects in Solving the Liquid Outflow Phenomena. *Langmuir* **2007**, *23*, 3230–3235.
36. Sheng, X.; Zhang, J.; Jiang, L. Application of the Restricting Flow of Solid Edges in Fabricating Superhydrophobic Surfaces. *Langmuir* **2009**, *25*, 9903–9907.
37. Zhang, J.; Wang, J.; Zhao, Y.; Xu, L.; Gao, X.; Zheng, Y.; Jiang, L. How Does the Leaf Margin Make the Lotus Surface Dry as the Lotus Leaf Floats on Water. *Soft Matter* **2008**, *4*, 2232–2237.
38. Ambravaneswaran, B.; Basaran, O. A. Effects of Insoluble Surfactants on the Nonlinear Deformation and Breakup of Stretching Liquid Bridges. *Phys. Fluids* **1999**, *11*, 997–1015.
39. Craster, R. V.; Matar, O. K.; Papageorgiou, D. T. Pinchoff and Satellite Formation in Surfactant Covered Viscous Threads. *Phys. Fluids* **2002**, *14*, 1364–1376.
40. Bhat, P. P.; Appathurai, S.; Harris, M. T.; Pasquali, M.; McKinley, G. H.; Basaran, O. A. Formation of Beads-on-a-String Structures during Break-up of Viscoelastic Filaments. *Nat. Phys.* **2010**, *6*, 625–631.
41. Murad, S.; Puri, I. K. Nanoscale Jet Collision and Mixing Dynamics. *Nano Lett.* **2007**, *7*, 707–712.
42. Gutmann, O.; Niekrawietz, R.; Kuehlewein, R.; Steinert, C. P.; Reinbold, S.; de Heij, B.; Daub, M.; Zengerle, R. Non-Contact Production of Oligonucleotide Microarrays Using the Highly Integrated TopSpot Nanoliter Dispenser. *Analyst* **2004**, *129*, 835–840.

43. de Heij, B.; Daub, M.; Gutmann, O.; Niekrawietz, R.; Sandmaier, H.; Zengerle, R. Highly Parallel Dispensing of Chemical and Biological Reagents. *Anal. Bioanal. Chem.* **2004**, *378*, 119–122.
44. Liimatainen, V.; Sariola, V.; Zhou, Q. Controlling Liquid Spreading Using Microfabricated Undercut Edges. *Adv. Mater.* **2013**, *25*, 2275–2278.
45. Byun, D.; Lee, Y.; Tran, S.; Nugyen, V.; Kim, S. Electrospray on Superhydrophobic Nozzles Treated with Argon and Oxygen Plasma. *Appl. Phys. Lett.* **2008**, *92*, 475–478.
46. Byun, D.; Lee, Y. Apparatus for jetting droplets using superhydrophobic nozzle. U.S. Patent 20090189952, 2009